OAK RIDGE NATIONAL LABORATORY LIBRARIES
3 4456 0555514 6

ORNL/TM-6999

ornl

OAK
RIDGE
NATIONAL
LABORATORY

UNION
CARBIDE

Fatigue Crack Propagation in Hastelloy X Weld Metal

T. Weerasooriya

OAK RIDGE NATIONAL LABORATORY
CENTRAL RESEARCH LIBRARY
CIRCULATION SECTION
4500N ROOM 175
LIBRARY LOAN COPY
DO NOT TRANSFER TO ANOTHER PERSON
If you wish someone else to see this report, send in name with report and the library will arrange a loan.
UCN-7969 (3 9-77)

OPERATED BY
UNION CARBIDE CORPORATION
FOR THE UNITED STATES
DEPARTMENT OF ENERGY

Printed in the United States of America. Available from
National Technical Information Service
U.S. Department of Commerce
5285 Port Royal Road, Springfield, Virginia 22161
NTIS price codes—Printed Copy: A03 Microfiche A01

This report was prepared as an account of work sponsored by an agency of the United States Government. Neither the United States nor any agency thereof, nor any of their employees, makes any warranty, expressed or implied, or assumes any legal liability or responsibility for any third party's use or the results of such use of any information, apparatus, product or process disclosed in this report, or represents that its use by such third party would not infringe privately owned rights.

ORNL/TM-6999
Distribution
Category UC-77

Contract No. W-7405-eng-26

METALS AND CERAMICS DIVISION

HTGR BASE TECHNOLOGY PROGRAM

GCR Structural Materials Studies (01332)

FATIGUE CRACK PROPAGATION IN HASTELLOY X WELD METAL

T. Weerasooriya

Date Published: November 1979

NOTICE This document contains information of a preliminary nature. It is subject to revision or correction and therefore does not represent a final report.

OAK RIDGE NATIONAL LABORATORY
Oak Ridge, Tennessee 37830
operated by
UNION CARBIDE CORPORATION
for the
U.S. DEPARTMENT OF ENERGY

OAK RIDGE NATIONAL LABORATORY LIBRARIES
3 4456 0555514 6

CONTENTS

ABSTRACT 1
INTRODUCTION 1
MATERIAL CHARACTERIZATION 2
Variables Governing Weldment Properties 3
Material 3
Joint design 5
Welding process and welding parameters 5
Postweld heat treatment 5
Soundness of the welds 5
Experimental procedure 6
RESULTS AND DISCUSSION 10
CONCLUSIONS 18
ACKNOWLEDGMENTS 21

FATIGUE CRACK PROPAGATION IN HASTELLOY X WELD METAL

T. Weerasooriya

ABSTRACT

The fatigue crack growth rate of Hastelloy X weld metal increased with stress intensity, temperature, and inverse frequency. The results were correlated with the equation

$$\frac{da}{dN} = (\Delta K)^n ,$$

for constant frequency or constant temperature. The values of A and n were computed with a linear regression algorithm. With decreasing frequency at constant ΔK and constant temperature (538°C) fatigue crack growth rates approach an upper limit. Fatigue crack growth rate of the weld metal was lower than that reported for base metal at 538°C and lower at 649°C for a frequency of 1 Hz.

INTRODUCTION

Hastelloy X, a Ni-Cr-Fe-Mo alloy (nominally 47, 23, 19, and 9 wt %, respectively), has been used successfully for more than two decades in elevated-temperature applications requiring both oxidation resistance and high strength. It is essentially a single-phase alloy with face-centered cubic structure. Strengthening is primarily by solid-solution alloying with the elements chromium, molybdenum, and tungsten. However, precipitation of carbide particles can additionally strengthen this alloy.

In the design of steam- and direct-cycle (gas turbine) High-Temperature Gas-Cooled Reactors (HTGRs), Hastelloy X has been suggested for fabrication of ducts that connect the reactor core to the steam generator or gas turbine section. Also, the alloy has been recommended for thermal barrier cover plates surrounding the reactor core. The nominal design temperature for hot ducts, which carry helium from the

reactor core to the steam generator section, is 788°C, with the possibility of random short-term variations of temperature up to 827°C. The design nominal temperature of the hot gas in the inlet of the hot ducts for gas turbine cycle HTGR is 816°C.[1,2] Hastelloy X is also one of the candidate materials for components of gas-cooled-reactor process heat plants. In these systems Hastelloy X could be used for ducting or for the tube or support-plate material of the intermediate and process heat exchangers.[1,2]

In the above applications fabrication procedures require welding in the construction of components, and the properties of the weldment could possibly differ from those of the base metal. Failures in weldments are often attributed to the growth of preexisting flaws from fatigue of these components. If one knows the rate of growth of subcritical cracks, the prediction of the life of components containing flaws is possible. This approach is particularly useful for design and safety analysis.

This document provides subcritical crack growth data on Hastelloy X weld metal. Test samples were obtained from weldments that were fabricated by welding two Hastelloy X plates with Hastelloy X filler metal.

MATERIAL CHARACTERIZATION

Specimens for this study were fabricated from solution-annealed 12.5-mm-thick Hastelloy X plates (heat 2600-4-4284) purchased from Cabot-Stellite. The mechanical properties of this heat are:

Heat treatment	solution-annealed at 1177°C followed by rapid cool
Ultimate tensile strength, MPa	790
0.2% yield strength, MPa	345
Elongation in 25 mm, %	49

The chemical composition of the Hastelloy X plates is:

Element	Content, wt %	Element	Content, wt %
Ni	Balance	Co	2.40
Cr	21.79	Mn	0.59
W	0.63	Mo	8.82
Fe	19.06	P	0.018
C	0.06	S	<0.005
Si	0.35	B	<0.002

Details of weldment fabrication are discussed later in this report. Figure 1 shows microstructures of the weldment. Second-phase microconstituents are probably carbides of the M_6C type with a lattice constant of 10.995 Å (ref. 3). In areas close to the fusion line, Hastelloy X base metal has a larger concentration of these coarse carbides [Fig. 1(b)].

Variables Governing Weldment Properties

Data obtained from one weldment may differ from the data obtained from another weldment for several reasons.

Material

Chemical composition can influence the elevated-temperature properties of a weldment.[4,5] Although the filler metal composition nominally dictates the composition of the weld metal, base metal dilution, fluxes, and cover gas all contribute to the final deposit composition. In this study chemical composition of the weld metal (heat 2600-4-4345) with 1.56-mm-diam Hastelloy X wire for filler is:

Element	Content, wt %	Element	Content, wt %
Cr	21.92	Ni	Balance
W	0.42	Mn	0.70
Fe	18.81	Mo	8.85
C	0.08	P	0.022
Si	0.40	S	<0.005
Co	2.09		

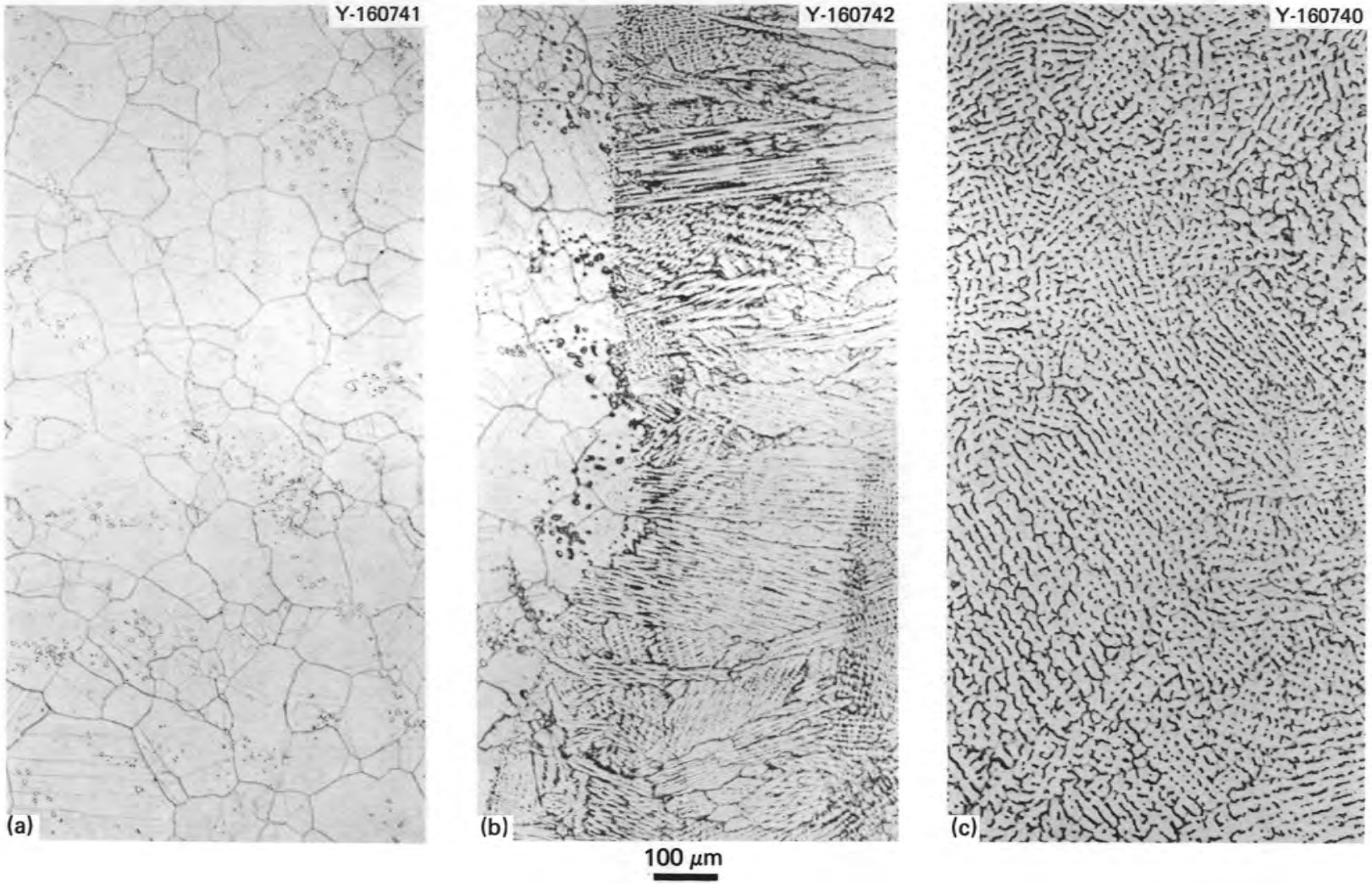

Fig. 1. Microstructures of the Hastelloy X Plates (Heat 2600-4-4284). (a) Solution-annealed base metal. (b) Weldment fusion zone. (c) Weldment weld metal.

Joint design

The geometry of the joint can lead to different residual stress patterns, structures, and properties of the welds. Weldments were fabricated with a V-groove of 75° included angle.

Welding process and welding parameters

The gas tungsten-arc (GTA), gas metal-arc (GMA), shielded metal-arc (SMA), and submerged-arc (SA) welding processes are most commonly used in joining nuclear power components. These processes can produce welds with different metallurgical structure and properties. Even with a given process, variation in welding parameters and techniques, such as current, voltage, travel speed, electrode size, number and sequence of passes, amplitude, frequency, polarity, and shape of applied voltage, may lead to different properties of the weldments.[4,6]

Weldments were made with the following parameters:

Welding process	GTA
Speed	3.75×10^4 mm/s (625 mm/min)
Voltage	9–9.5 V
Passes	7
Current	195 A
Straight polarity	
Electrode	2.34 mm in diameter, 30° included angle

Postweld heat treatment

Welds in nuclear applications are heat-treated many times to alter metallurgical structure or to relieve residual stresses. However, the weldment that was fabricated for testing in this program was not post-weld heat-treated.

Soundness of the welds

Defects, such as inclusions, porosity, and incomplete fusion, can degrade the properties. The weldment was radiographed, and no defects were indicated.

Experimental procedure

Standard (ASTM E 647) compact tension (CT) specimens were prepared from weldments that were fabricated as outlined above. The dimensions of the specimens are given in Fig. 2. The notched area of the specimen was located at the center of the weld metal such that the major axis of the weldment coincided with the major axis of the notch. The base metal was oriented such that the rolling direction was perpendicular to the plane of crack growth.

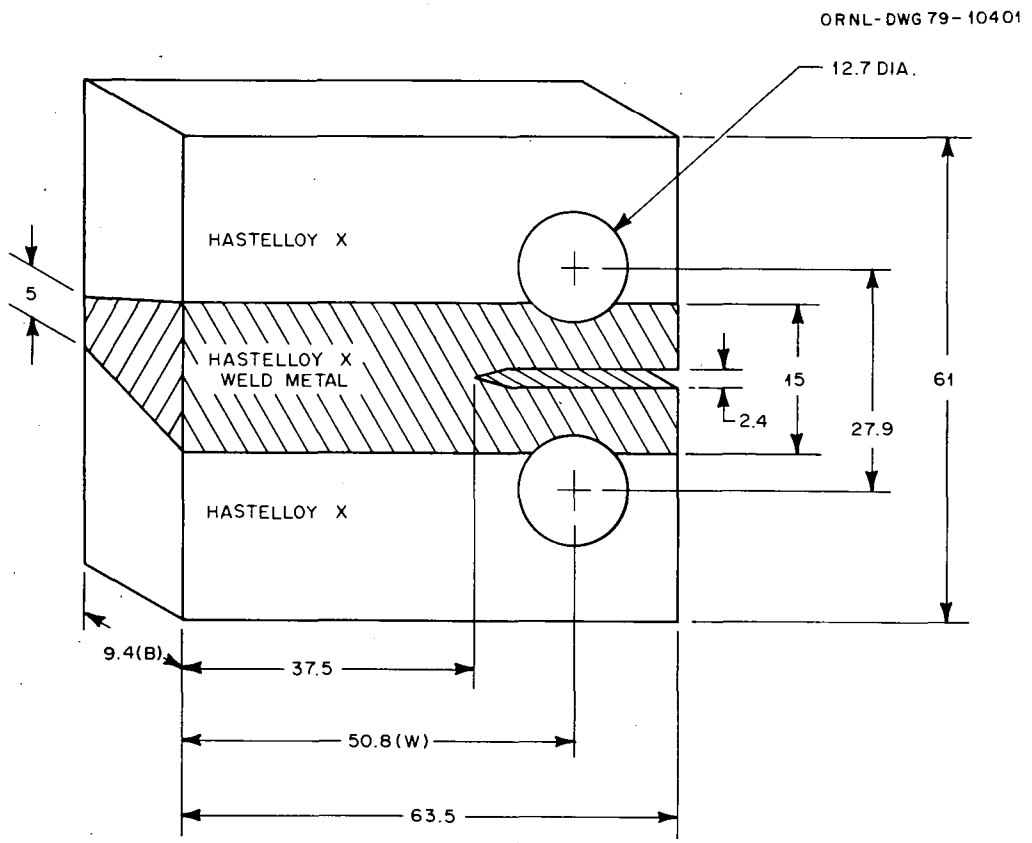

Fig. 2. Dimensions in Millimeters of the Compact Tension (CT) Specimen with the Weldment.

Specimens were precracked at room temperature with a servo-hydraulic testing machine. Precracking was performed with a sinosoidal waveform and was terminated when a value for maximum stress intensity

(K_{max}) slightly smaller than the initial K_{max} for the tests was reached. The ratio (R) of K_{min} to K_{max} was kept at 0.05 throughout all the tests.

The machine setup used for elevated-temperature fatigue growth testing is shown in Figs. 3 and 4. All tests were conducted on a closed-loop, servo-controlled electrohydraulic MTS testing machine, employing a triangular waveform. The tests were conducted in air with a stress ratio value (P_{min}/P_{max}) of R = 0.05 (according to ASTM E 647, unless stated otherwise). Induction heating maintained the elevated temperature during fatigue testing. Specimen temperature was controlled to ±1°C, while the temperature variation along the path of the crack was less than 6°C. Crack lengths were measured optically with traveling microscopes at periodic intervals.

Crack growth rates were computed by fitting a continuous cubic spline curve to the average crack length data.[7] The closeness of the

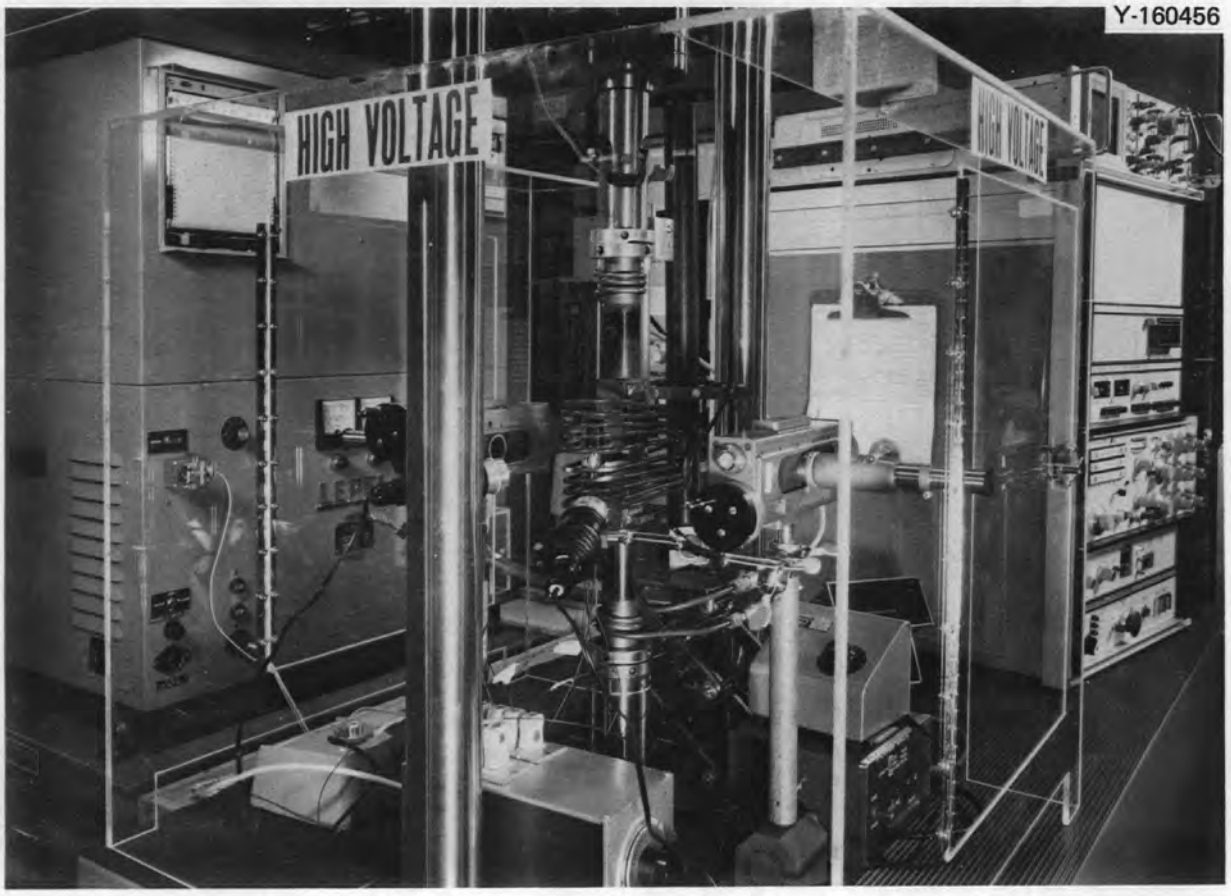

Fig. 3. The Testing Machine. Induction heating was used to maintain temperature.

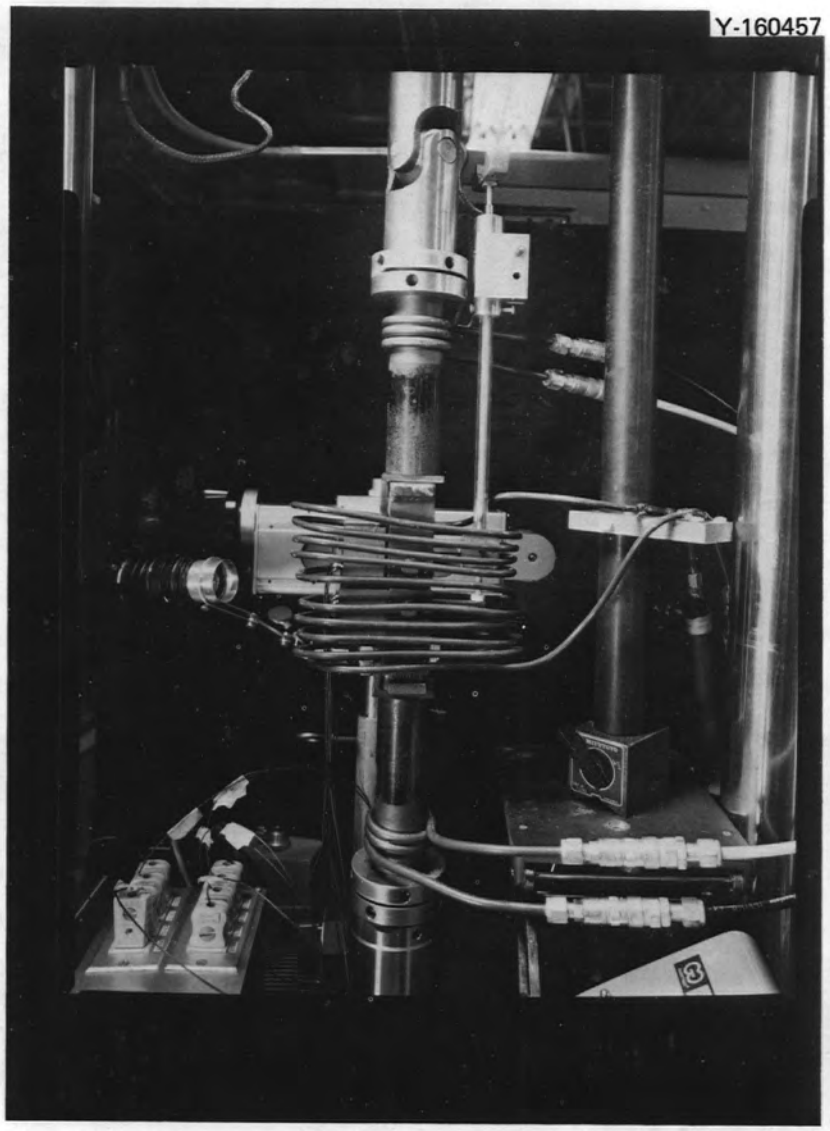

Fig. 4. Close-up of Heating Coil in Testing Machine.

fitted cubic spline curve to the experimental points was determined by the variable S in Eq. (1):

$$\sum_{i=1}^{N} [ai - ai(\text{fit})]^2 = S^2 N \ , \tag{1}$$

where

ai = measured crack length, and

$ai(\text{fit})$ = fitted crack length.

The spline curve was fitted to satisfy the above equation. In this analysis S was taken as 0.025 mm and can be considered as a measure of the confidence of the optical readings. The stress intensity expression used to calculate ΔK was as follows:

$$\Delta K = \frac{\Delta P}{B\sqrt{W}}\left[29.6\left(\frac{a}{W}\right)^{0.5} - 185.5\left(\frac{a}{W}\right)^{1.5} + 655.7\left(\frac{a}{W}\right)^{2.5} - 1017\left(\frac{a}{W}\right)^{3.5} + 638.9\left(\frac{a}{W}\right)^{4.5}\right], \tag{2}$$

where

ΔP = cyclic load range (i.e., $P_{max} - P_{min}$),

a = crack length,

B = specimen thickness, and

W = specimen width.

The tests were terminated at the onset of permanent crack opening.

A computer code was prepared and used to calculate growth rates and plot growth vs ΔK, as discussed above. The computer code will fit a least squares regression line for da/dN vs ΔK plots and calculate A and n in the equation

$$\frac{da}{dN} = A(\Delta K)^n , \tag{3}$$

where

$\frac{da}{dN}$ = crack growth in mm/cycle, and

ΔK = stress intensity in MPa$\sqrt{m}$ for each plot.

We conducted tests to find the variation of subcritical crack growth rates with varying temperatures at 1 Hz. Tests were conducted at 538, 650, and 760°C. Also, tests were conducted to find the behavior of crack growth rates with frequencies of 0.1, 1, and 10 Hz at 538°C.

RESULTS AND DISCUSSION

We correlated crack growth data with Eq. (3). Figures 5 through 7 give the da/dN vs ΔK data on logarithmic coordinates for the tests conducted to find out the effect of temperature on fatigue crack growth rates for a constant frequency. These figures also give both the linear regression lines for these data and the values of A and n in Eq. (3) (da/dN — mm/cycle; ΔK — MPa$\sqrt{m}$) for the regression lines. The scatter band for weld metal is on the order of plus or minus twice the predicted values by the regression line. This probably resulted from the anisotropy and inhomogeniety of the weld metal. Figure 8 gives a comparison of the variation of fatigue crack growth rate with temperature at 1 Hz. As observed for most of the materials, crack growth rate increases with increasing temperature for Hastelloy X weld metal. One explanation is that as temperature increases deterioration of the crack tip from oxidation is higher. However, at higher stress intensities differences in crack growth rates from temperature become smaller. At higher growth rates unoxidized metal is rapidly exposed, and hence oxidation at the crack tip has little effect on growth rate. Figures 5 and 6 compare the fatigue crack growth rates of weld metal and base metal. At both 538 and 650°C base metal has a higher crack growth rate compared to that of weld metal. At 650°C the difference of the fatigue crack growth rates of base metal and weld metal increases with increasing stress intensity factor.

Figures 9 and 10 give the fatigue crack growth rate data, fitted regression line, and values of A and n for further tests conducted on weld metal to find the effect of frequency on fatigue crack growth rates at 538°C. Figure 11 compares the effect of frequency on fatigue crack growth rate of weld metal at 538°C. In general, the fatigue crack growth rate increases with decreasing frequency. In the range of frequencies between 0.1 and 1 Hz, the difference in the fatigue crack growth rate (FCGR) is not substantial, but the difference in crack growth rates between the frequencies of 10 and 0.1 Hz or 10 and 1 Hz is greater.

ORNL-DWG 78-18702R

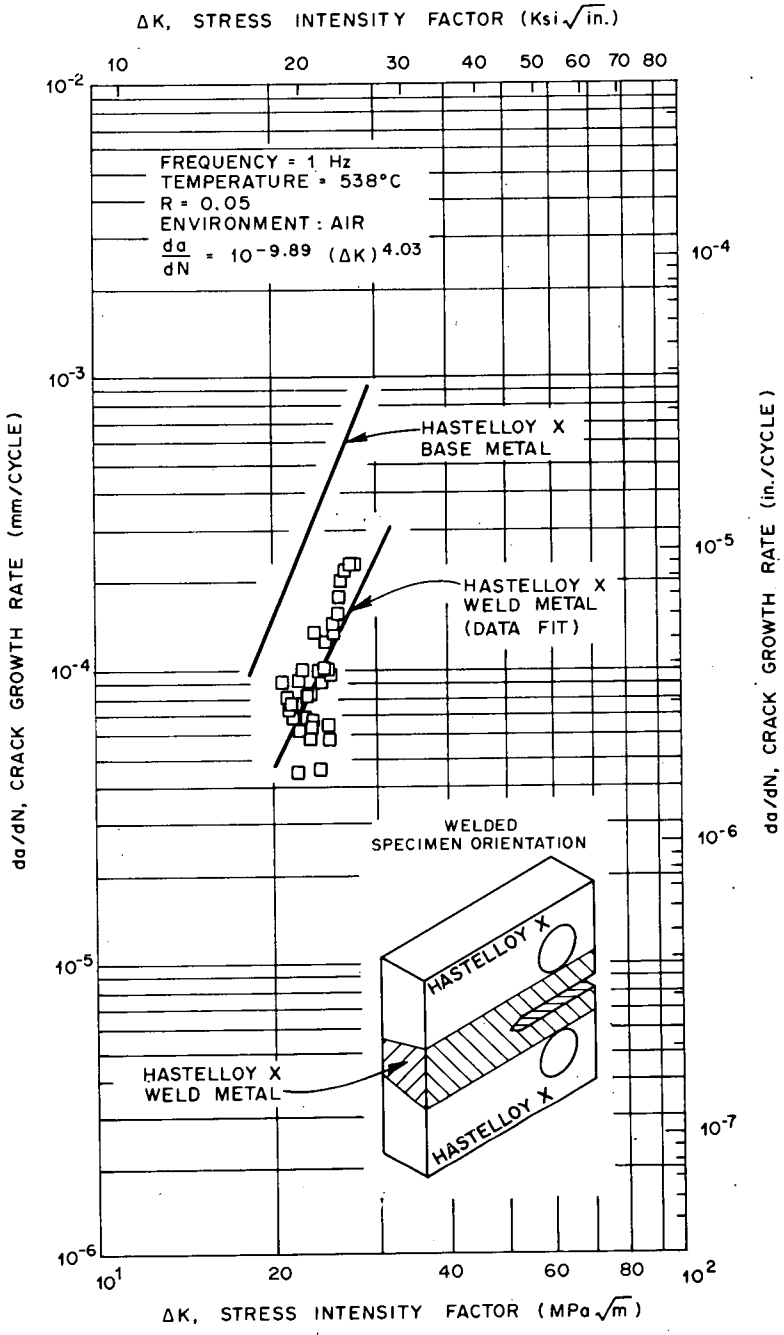

Fig. 5. Fatigue Crack Growth Rate of Hastelloy X Weld Metal at 538°C and 1 Hz. Base metal data is from: C. R. Brinkman et al., *Application of Hastelloy X in Gas-Cooled Reactor Systems,* ORNL/TM-5405 (October 1976). Note that SI units were employed in the development of the above equation.

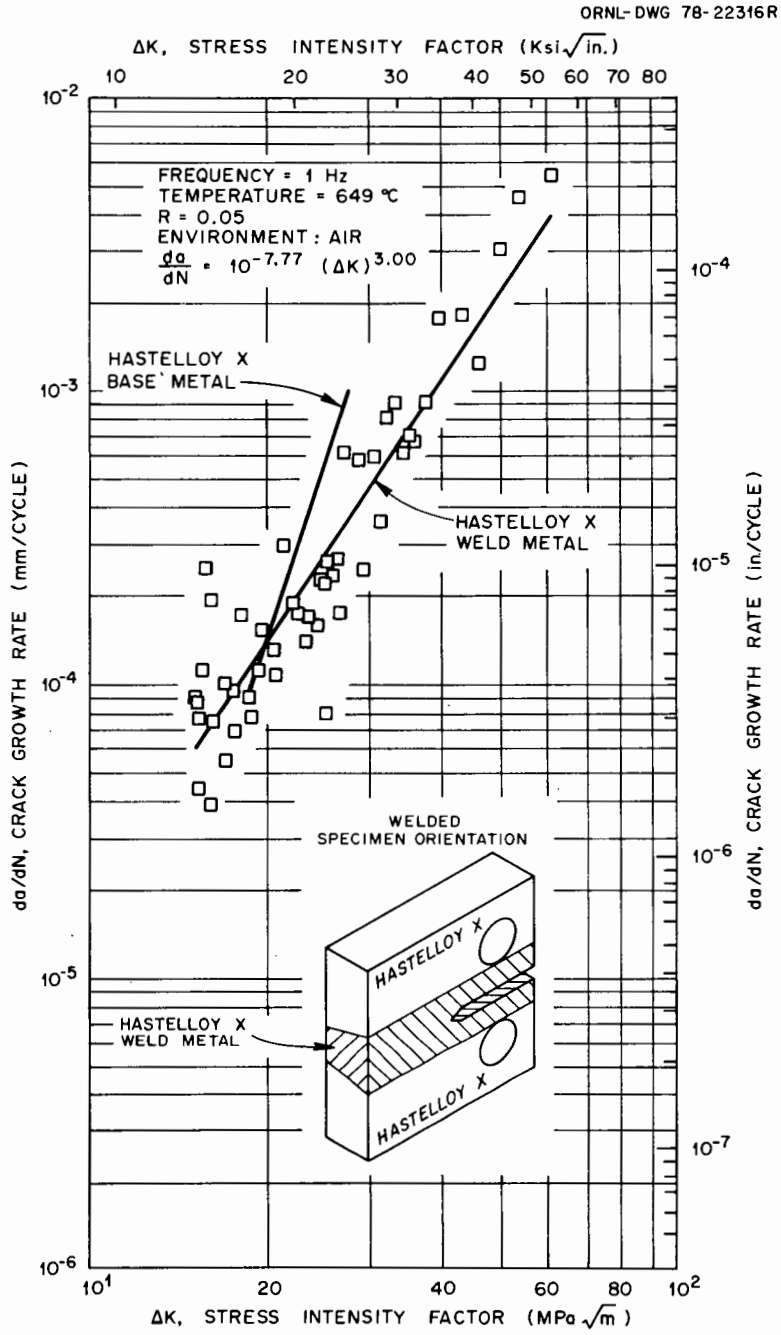

Fig. 6. Fatigue Crack Growth Rate of Hastelloy X Weld Metal at 649°C and 1 Hz. Base metal data is from: C. R. Brinkman et al., *Application of Hastelloy X in Gas-Cooled Reactor Systems*, ORNL/TM-5405 (October 1976).

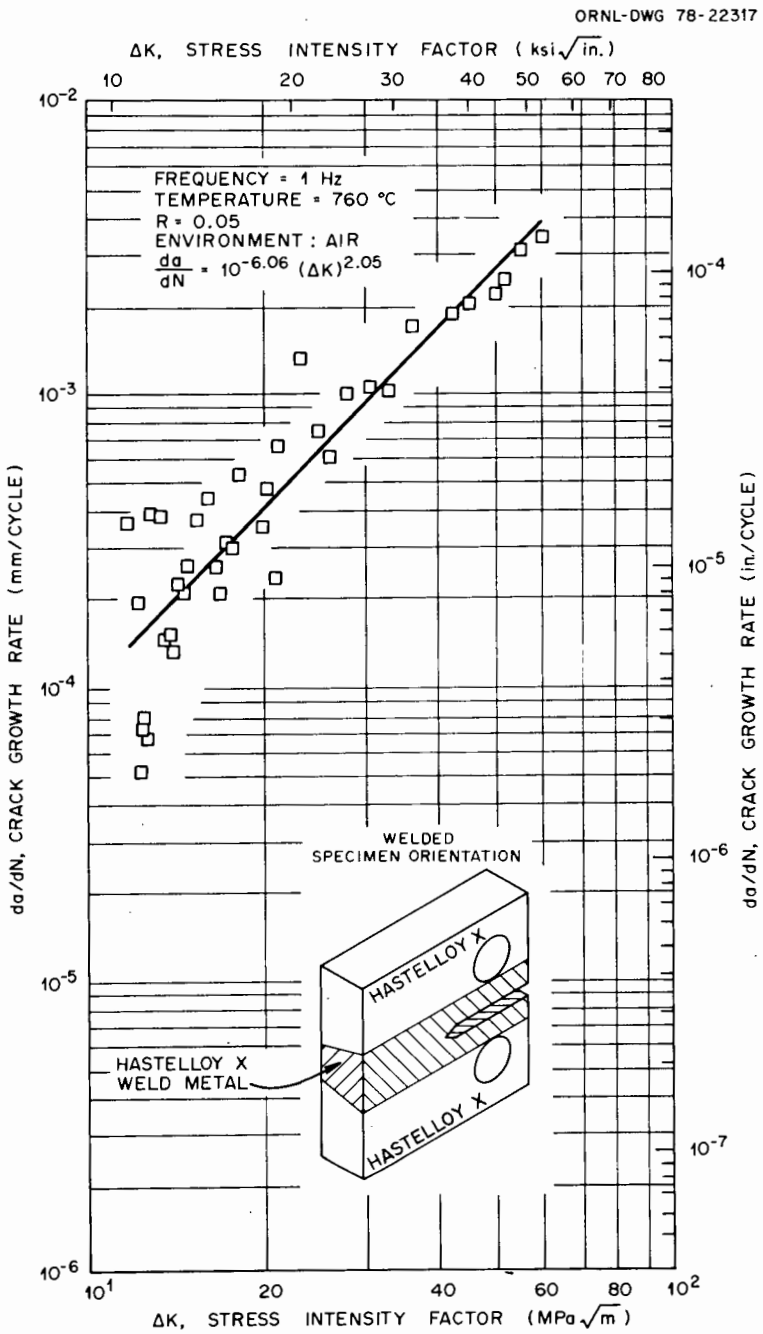

Fig. 7. Fatigue Crack Growth Rate of Hastelloy X Weld Metal at 760°C and 1 Hz.

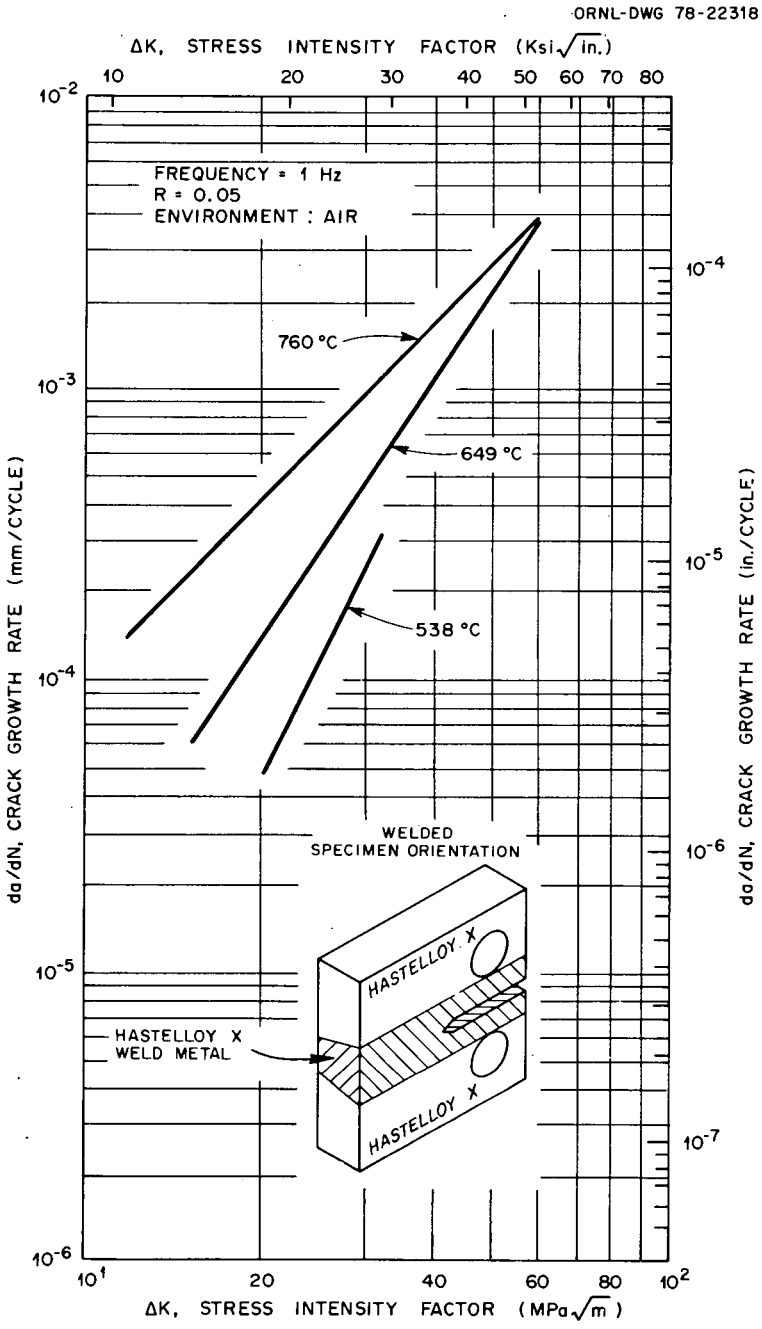

Fig. 8. Effect of Temperature on Fatigue Crack Growth Rate of Hastelloy X Weld Metal at 1 Hz.

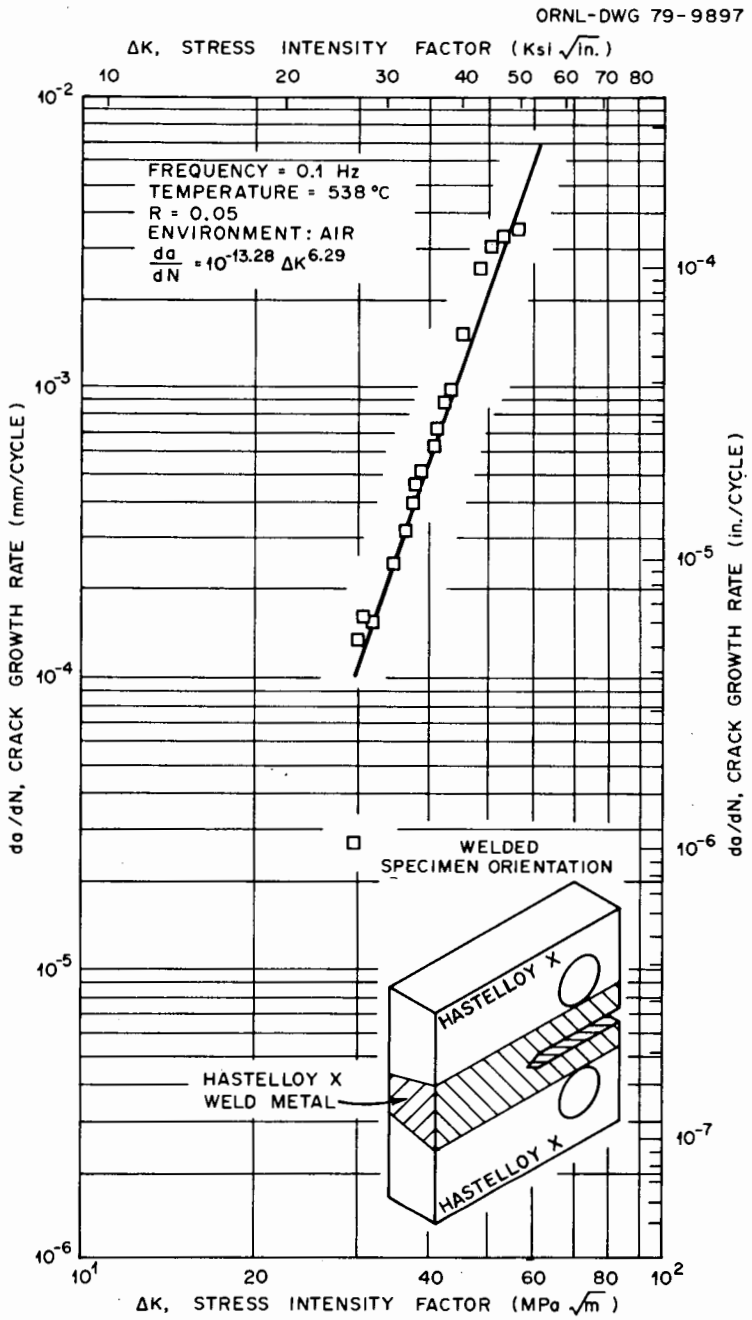

Fig. 9. Fatigue Crack Growth Rate of Hastelloy X Weld Metal at 538°C and 0.1 Hz.

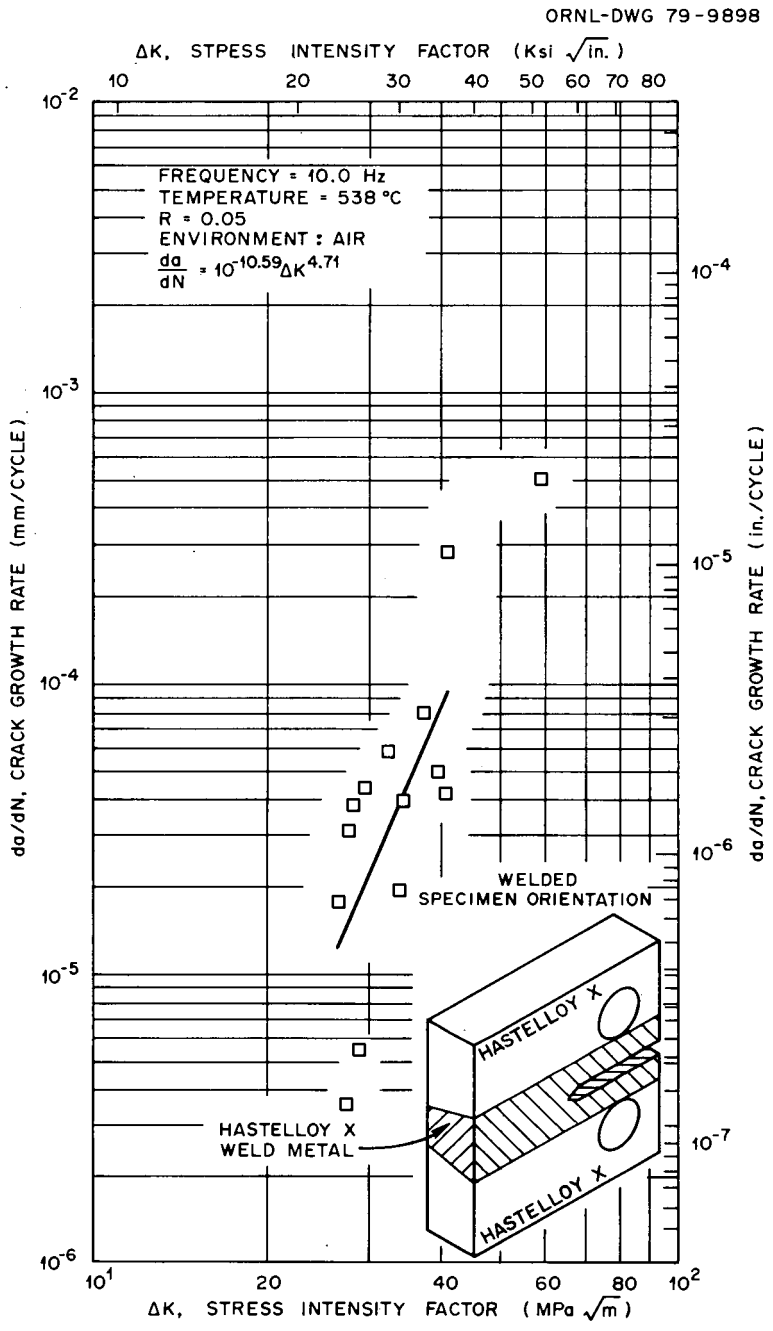

Fig. 10. Fatigue Crack Growth Rate of Hastelloy X Weld Metal at 538°C and 10 Hz.

ORNL-DWG 79-9250

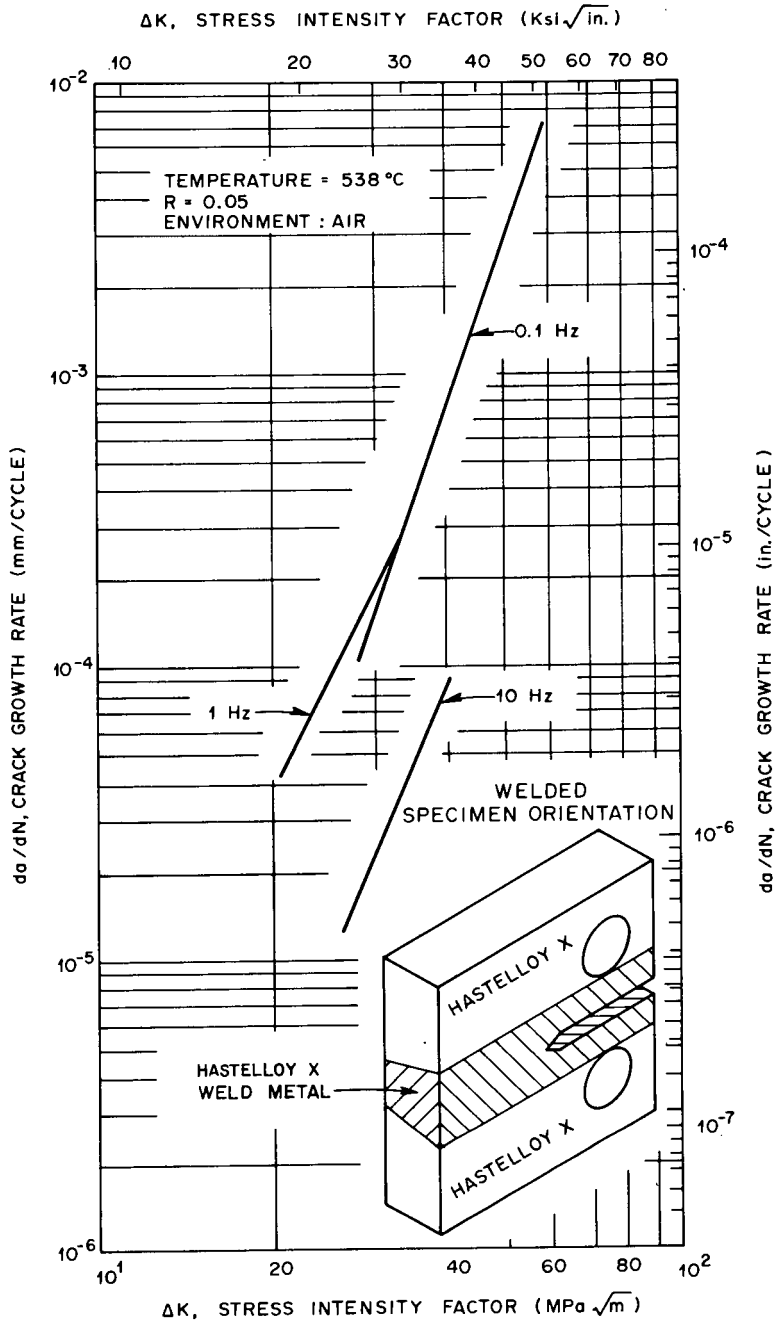

Fig. 11. Effect of Frequency on Fatigue Crack Growth Rate of Hastelloy X Weld Metal at 538°C.

The principal causes of the effect of frequency are again believed to be: (1) the increased oxidation at the crack tip, and (2) the transient creep that occurs during the longer cycle periods at the lower frequencies. There appears to be an upper limit of crack growth rate for decreasing frequency. When the frequency is reduced there may be a stage at which increased environmental attack is balanced by the blunting and stress relaxation at the crack tip and hence a reduction of the driving force ΔK at the crack tip. Figure 12 shows representative areas of the fracture surface. These clearly show the fatigue-induced striations on the crack surface and how these striation configurations seem to differ. This is expected as weld metal does not have a homogeneous structure (as a result of multipass welding, including oscillation in any given pass).

Figure 13 shows a typical orientation of the fatigue crack with respect to the microstructure of the weld metal. Correlation of crack configuration and microstructural details was not detected, though on a few occasions the crack tends to change direction to make the dendrites parallel in the structure.

CONCLUSIONS

This report presents the results of part of a broad program of study on FCGR properties for HTGR applications. We discussed results of the characterization of fatigue crack growth in air for Hastelloy X weld metal. We concluded the following from the results:

1. The FCGR in weld metal increases with increasing temperature at 1 Hz in the range 538 to 760°C.

2. The FCGR for weld metal decreases with increasing frequency from 1 to 10 Hz at 538°C. Also, there is an upper limit growth rate for decreasing frequency at a constant ΔK value.

3. The FCGR of base metal is higher than that of weld metal both at 538 and 649°C for frequency of 1 Hz.

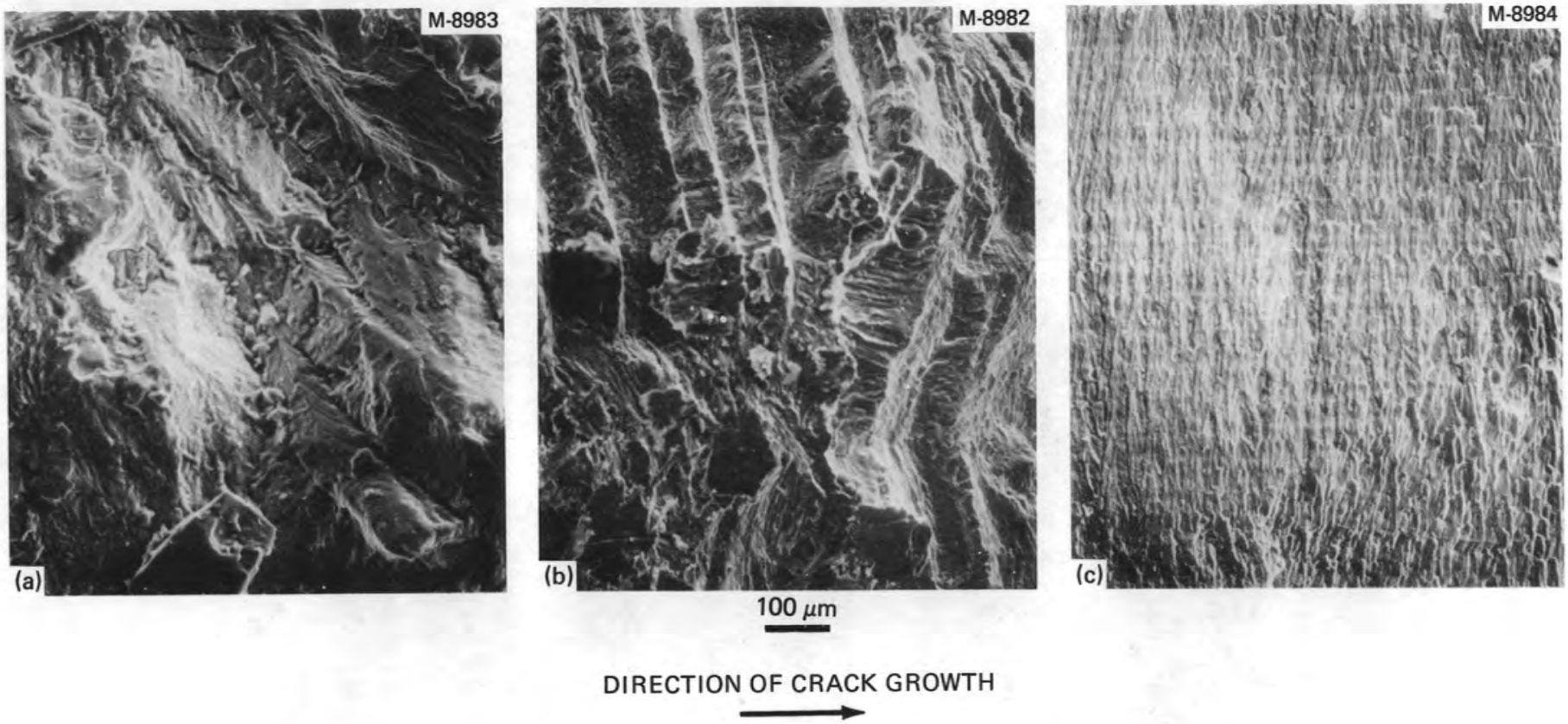

Fig. 12. Three Different Types of Fracture Surfaces in Fatigue Crack Growth Testing for Hastelloy X Weld Metal. These were typical on all the specimens tested. Correlation between crack growth parameters does not exist.

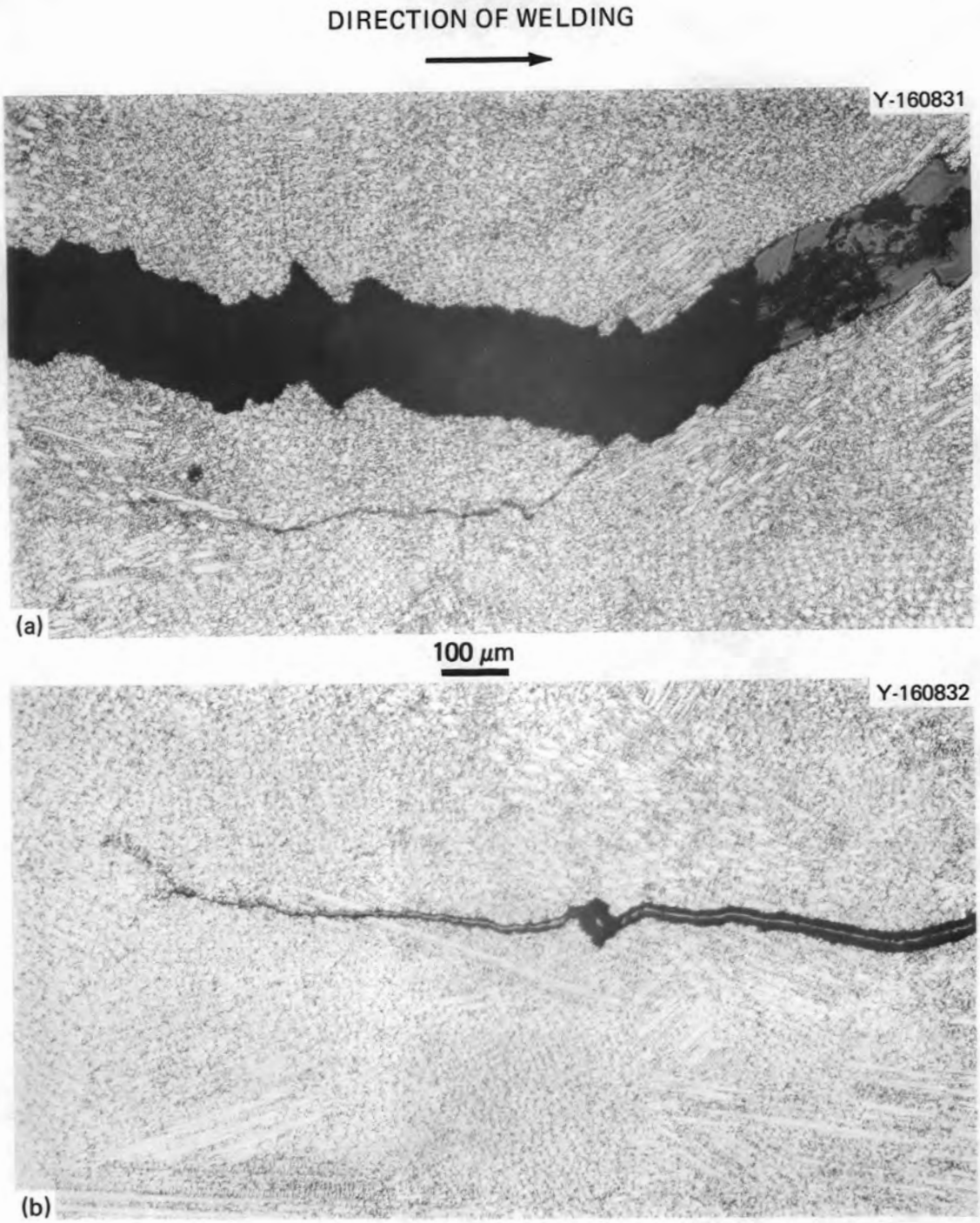

Fig. 13. Orientation of Two Locations of a Typical Fatigue Crack with Respect to the Microstructure.

ACKNOWLEDGMENTS

The author gratefully appreciates the help and patience shown by J. P. Strizak during the initiation period of this testing program.

The report was reviewed by M. K. Booker and R. W. Swindeman, edited by B. G. Ashdown, and prepared for final publication by P. T. Thornton.

REFERENCES

1. P. L. Rittenhouse, *Initial Assessment of the Status of HTGR Metallic Structural Materials Technology,* ORNL/TM-4760 (December 1974).
2. C. R. Brinkman et al., *Application of Hastelloy X in Gas-Cooled Reactor Systems,* ORNL/TM-5405 (October 1976).
3. G. Y. Lai, "An Investigation of the Thermal Stability of a Commercial Ni-Cr-Fe-Mo Alloy (Hastelloy X)," *Metall. Trans. A* 9A: 827–33 (1978).
4. R. T. King, D. A. Canonico, and C. R. Brinkman, "Elevated-Temperature Weldment Behavior as Related to Nuclear Design Criteria," *Weld. J. (Miami)* 54(8): 265-s–275-s (August 1975).
5. F. C. Hull, "The Effect of Composition on the Stress-Rupture Properties of Fully Austenitic Stainless Steel Weld," paper presented at First National Congress on Pressure Vessels and Piping, San Francisco, Calif., May 10–12, 1971.
6. G. M. Goodwin, N. C. Cole, and G. M. Slaughter, "A Study of Ferrite Morphology in Austenitic Stainless Steel Weldments," *Weld. J. (Miami)* 51(9): 425-s–429-s (September 1972).
7. T. Weerasooriya, *Fatigue Crack Propagation in the Heat-Affected Zone of 2 1/4 Cr-1 Mo Steel and ERNiCr-3 Weldments — Interim Report,* ORNL/TM-6971 (in press).

ORNL/TM-6999
Distribution Category UC-77

INTERNAL DISTRIBUTION

1–2. Central Research Library
3. Document Reference Section
4–5. Laboratory Records Department
6. Laboratory Records, ORNL, R.C.
7. ORNL Patent Section
8. M. K. Booker
9. C. R. Brinkman
10. C. W. Collins
11. B. E. Foster
12. G. M. Goodwin
13. M. L. Grossbeck
14–16. M. R. Hill
17. J. A. Horak
18. R. R. Judkins
19. P. R. Kasten
20. E. H. Lee
21. K. C. Liu
22. H. E. McCoy
23. R. K. Nanstad
24. P. L. Rittenhouse
25. G. M. Slaughter
26. J. H. Smith
27–31. J. P. Strizak
32. R. W. Swindeman
33. V. J. Tennery
34. F. W. Wiffen
35. R. W. Balluffi (Consultant)
36. A. L. Bement, Jr. (Consultant)
37. W. R. Hibbard, Jr. (Consultant
38. E. H. Kottcamp, Jr. (Consultan
39. M. J. Mayfield (Consultant)
40. J. T. Stringer (Consultant)

EXTERNAL DISTRIBUTION

41–42. DOE, DIVISION OF NUCLEAR POWER DEVELOPMENT, Washington, DC 20545

Director

43. SAN-DEVELOPMENT, SAN DIEGO AREA OFFICE, P.O. Box 81325, San Diego, CA 92138

Senior Program Coordinator

44. DOE SAN FRANCISCO OPERATIONS OFFICE, 1333 Broadway, Wells Fargo Building, Oakland, CA 94612

Manager

45–46. DOE, OAK RIDGE OPERATIONS OFFICE, P.O. Box E, Oak Ridge, TN 37830

Assistant Manager, Energy Research and Development

Director, Nuclear Research and Development

47–219. DOE, TECHNICAL INFORMATION CENTER, P.O. Box 62, Oak Ridge, TN 37830

For distribution as shown in TID-4500 Distribution Category, UC-77 (Gas-Cooled Reactor Technology).

☆ U. S. GOVERNMENT PRINTING OFFICE: 1979-640-245-294